Monatshefte für Chemie 133, 873–887 (2002)

Monatshefte für Chemie
Chemical Monthly

Influence of Al_2O_3 Nanoparticles on the Thermal Stability of Ultra-Fine Grained Copper Prepared by High Pressure Torsion

Jakub Čížek[1,a,*], **Ivan Procházka**[1], **Radomír Kužel**[1], and **Rinat K. Islamgaliev**[2]

[1] Faculty of Mathematics and Physics, Charles University, CZ-18000 Prague, Czech Republic
[2] Institute of Physics of Advanced Materials, Ufa State Aviation Technical University, Ufa 450000, Russia

Summary. Ultra-fine grained (UFG) Cu (grain size 80 nm) containing 0.5 wt.% Al_2O_3 nanoparticles (size 20 nm) was prepared by high pressure torsion (HPT). Positron lifetime spectroscopy was employed to characterize the microstructure of this material, especially with respect to types and concentration of lattice defects. The evolution of microstructure with increasing temperature was studied by positron lifetime spectroscopy and X-ray diffraction measurements. The thermal stability of the Cu + 0.5 wt.% Al_2O_3 nanocomposite was compared with that of pure UFG Cu prepared by the same technique. The processes taking place during thermal recovery of the initial nanoscale structure in both studied materials are described.

Keywords. Nanostructures; Spectroscopy; Positron annihilation.

Introduction

Recently it has been found that ultra-fine grained (UFG) materials can be produced using severe plastic deformation. Grain sizes from 50 to 150 nm in metals were achieved by high pressure torsion (HPT) [1, 2]. The equal channel pressing technique (ECAP) [1] represents another method based on the above phenomenon. The UFG materials prepared by ECAP exhibit grain sizes of about 200 nm [3]. However, more massive samples can be prepared by ECAP, whereas the size of the samples prepared by HPT is limited [3]. Smaller grain sizes can be produced by HPT; therefore, this method was choosen for the preparation of the samples in this work. In comparison with other techniques of preparation of nanocrystalline

* Corresponding author. E-mail: jcizek@mbox.troja.mff.cuni.cz
[a] Current address: Institut für Materialphysik, Universität Göttingen, D-37073 Göttingen, Germany

materials (*e.g.* gas condensation or ball milling), HPT and ECAP are capable of producing high-purity specimens with no residual porosity.

TEM investigation of UFG Cu and Ni prepared by HPT [4, 5] have revealed a fragmented structure with high-angle misorientation of neighboring grains. Dislocations are concentrated in distorted layers along grain boundaries (GBs), whereas the grains themselves are almost free of dislocations. A highly non-uniform distribution of dislocations was also confirmed by XRD [6]. Most of the GBs are in non-equilibrium states of higher energy. The specific structure of UFG materials leads to a number of unusual physical and mechanical properties. In particular, the UFG materials exhibit abnormally high diffusion activity [7], unusual changes in *Curie* temperature, saturation magnetization, and elastic properties [8]. Moreover, the UFG materials are characterized by combination of high strength and ductility [1, 9]. These advantageous mechanical properties make them highly attractive for further industrial applications.

Valuable information about defects in UFG materials has been obtained by means of positron lifetime (PL) spectroscopy [5, 10]. Two types of defects were found in UFG Cu: (*i*) dislocations inside the distorted regions near to GBs and (*ii*) microvoids consisting of a few vacancies distributed homogeneously throughout the grains.

The evolution of UFG structures with increasing temperature is interesting from a physical point of view as one obtains information about the thermal recovery of the highly non-equilibrium initial structure. Moreover, detailed knowledge about thermal stability is necessary for further industrial applications of these materials. It has been found that thermal recovery of UFG structures is realized by abnormal grain growth followed by recrystallization, *i.e.* grain growth in the whole volume of the sample [5, 11]. Recently, it has been proposed that ceramic nanoparticles may inhibit the grain growth and, thereby, extend the thermal stability of the UFG structure. Indeed, investigations of UFG Cu with 0.5 wt.% Al_2O_3 have revealed enhanced thermal stability of this nanocomposite compared to pure UFG Cu [12, 13]. The onset of the recrystallization was shifted from 170°C in pure UFG Cu [4] to 400°C in UFG Cu + 0.5 wt.% Al_2O_3 [12]. However, relaxation of elastic strain and some recovery of defects indicated by a decrease of the electrical resistance precede the recrystallization [12]. Changes of microstructure corresponding to this recovery remain still unclear, but it is believed that they are connected with some changes of defect structure. PL spectroscopy represents an important tool for the investigation of these changes due to its high sensitivity to open volume defects [14].

In the present work, the thermal evolution of the microstructure of UFG Cu + 0.5 wt.% Al_2O_3 prepared by HPT was studied by PL spectroscopy and XRD, the main attention being focused on changes of the defect structure. The obtained results were compared with those for pure UFG Cu prepared by the same technique.

Results and Discussion

As-prepared state

The PL spectrum of pure UFG Cu can be fitted best by three exponential components; the lifetimes and relative intensities of these components are shown

Table 1. Positron lifetimes and corresponding relative intensities ($I_1 + I_2 + I_3 = 100\%$) for as-prepared UFG Cu and UFG Cu + 0.5 wt.% Al_2O_3; the values in parentheses represent the measurement errors (one standard deviation)

Specimen	τ_1 (ps)	I_1 (%)	τ_2 (ps)	I_2 (%)	τ_3 (ps)	I_3 (%)
Pure UFG Cu	67(8)	3.3(5)	166(2)	72(2)	255(2)	25(1)
UFG Cu + 0.5 wt.% Al_2O_3	–	–	161(3)	60.4(5)	257(1)	39.6(5)

in Table 1. The shortest component's lifetime τ_1 is well below 100 ps; this is remarkably lower than the lifetime of positrons in defect-free Cu which amounts to 114.5 ± 0.1 ps [10]. It is well known that when open volume defects are present, the lifetime of free positrons is shortened due to positron trapping at the defects [14]. The lifetimes of positrons trapped at open volume defects are always higher than the lifetimes of free positrons in defect-free material. Thus, the component of lifetime τ_1 can be obviously attributed to free positrons. The small relative intensity of this component clearly indicates that the majority of positrons annihilate from trapped states at defects. The lifetime τ_2 of the second component corresponds to the lifetime of 164 ps of positrons trapped at dislocations [15, 16]. This component originates from positrons trapped at dislocations in distorted regions along GBs; for a detailed discussion, see Refs. [5, 10]. The third component (lifetime τ_3) represents a contribution of positrons trapped at microvoids inside grains [5, 10]. Using theoretical calculations in Ref. [5], one obtains a size of the microvoids in the as-prepared specimen corresponding to 5 monovacancies, meaning that the diameter of the microvoids is about 0.5 nm. Some rare microvoids were found by TEM inside grains in pure UFG Cu [5]. The formation of microvoids of similar size was observed by PL spectroscopy also on plastically deformed polycrystalline Cu [16]. It is reasonable to assume that there is some size distribution of the microvoids, and only the largest microvoids are visible by TEM. In principle, there is no reason why the microvoids cannot be situated also inside the distorted regions. To solve this question we used the diffusion model of positron behaviour in UFG materials as described in Ref. [5]. A detailed description of the diffusion model is out of the scope of the present work; therefore, we give here only the basic ideas of the model and we will discuss the results of its application. We assume that a UFG or a nanocrystalline material consists of spherical non-distorted regions (grain interiors) with radius R which are separated by distorted regions of thickness δ. The dislocation density inside the non-distorted regions is below the detection limit of PL spectroscopy (about $10^{12}\,m^{-2}$). On the other hand, the distorted regions are characterized by high dislocation density. Thus, we assume that positrons annihilate from trapped states at dislocations inside the distorted regions only. Contrary to coarse-grained materials, the volume fraction of the distorted regions cannot be neglected in the UFG and the nanocrystalline materials. Therefore, the positrons are divided into two groups:

1) positrons which end their thermalization inside the distorted regions (we assume that they are trapped at dislocations there) and

2) positrons which end their thermalization inside the non-distorted regions; these may a) annihilate from the free state, b) be trapped in microvoids, or c) diffuse to distorted regions and be trapped at a dislocation there.

To solve this problem one has to solve the positron diffusion equation which was done similar to *Dupasquier et al*. [17]. As a result we obtained density of free positrons $n(\mathbf{r}, t)$ at a given time t and at position $\mathbf{r}$. From the density of the free positrons one can calculate the densities of the positrons trapped at the defects and deduce the shape of a PL spectrum which can be directly fitted to the shape of the experimental one. As a consequence, we can determine the linear size of the non-distorted regions, $2R$, which corresponds to the coherent domain size [5], the volume fraction of the distorted regions, η, and the density of the dislocations and concentration of the microvoids.

Regarding the microvoids, we used two different approaches in the diffusion model: (*i*) we assumed that the microvoids are distributed homogeneously inside grains only, *i.e*. they are not situated inside the distorted regions, and (*ii*) in an alternative approach the microvoids were assumed to be distributed homogeneously throughout the whole material, *i.e*. also inside the distorted regions. Approach (*ii*) leads to unphysically small grain sizes (below 10 nm), whereas approach (*i*) gave the grain sizes plotted in Fig. 9 and listed in Table 2 and which agree well with the coherent domain sizes determined by XRD. Thus, we conclude that the assumption that the microvoids are situated inside grains only is much more realistic, and approach (*i*) was used for elaboration of PL data in this work. For a detailed description of both approaches, see Ref. [5].

Two components were resolved in UFG Cu + 0.5 wt.% Al_2O_3 (see Table 1). Similarly to pure UFG Cu, the component with lifetime $\tau_2 = 161$ ps results from positrons trapped at dislocations inside the distorted regions, whereas the component with $\tau_3 = 257$ ps represents a contribution of positrons trapped at the microvoids inside grains. No free positron component was found in UFG Cu + 0.5 wt.% Al_2O_3. This may be a consequence of smaller grain size, as the relative intensity of this component is very small even in pure UFG Cu.

Whereas the lifetimes of trapped positrons are virtually the same for both specimens, the relative intensity of the component originating from the microvoids is remarkably higher for UFG Cu + 0.5 wt.% Al_2O_3. Thus, the size of the microvoids is the same in both specimens, but their concentration is higher in UFG Cu + 0.5 wt.% Al_2O_3.

Table 2. The coherent domain size a obtained by XRD and the size of the non-distorted regions $2R$ calculated from PL spectra using the diffusion model [5]; for comparison, the mean grain size d determined by TEM [4, 12] is included; the values in parentheses represent the measurement errors (one standard deviation)

Specimen	a (nm)	$2R$ (nm)	d (nm)
Pure UFG Cu	80(10)	80(4)	107
UFG Cu + 0.5 wt.% Al_2O_3	50(10)	64(4)	80

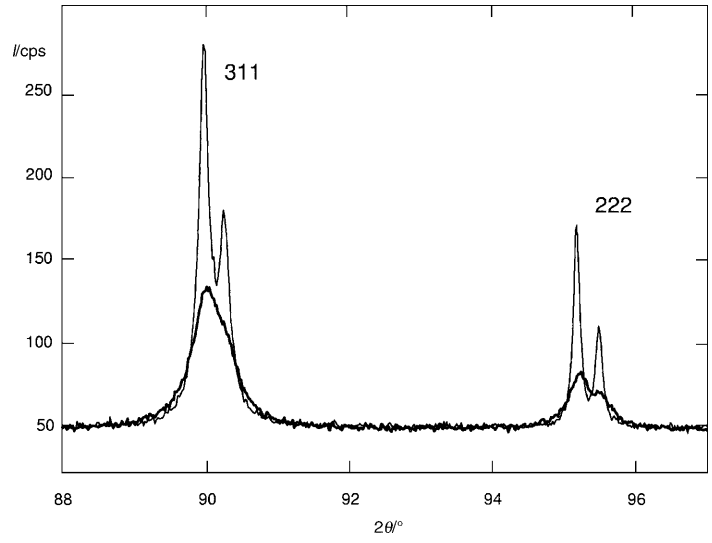

Fig. 1. XRD profiles (311) and (222) for UFG Cu with 0.5 wt.% Al_2O_3 after preparation (thick line) and after annealing at 550°C (thin line)

The lattice parameter determined for the pure UFG specimen by XRD measurements (3.6152 Å) agrees well with the values given for PDF-2 [18] (3.6150 Å). This means the absence of both impurities in the lattice and residual stresses. Texture indices show a random grain distribution or a weak (111) texture which does not vary with annealing temperature. The texture does not change during the recrystallization.

A typical feature of the XRD spectra for both UFG specimens is a broadening of the diffraction profiles which decreases with annealing temperature. This is illustrated in Fig. 1, where the measured XRD peaks (311) and (222) for as-prepared UFG Cu + 0.5 wt.% Al_2O_3 and for the specimen after annealing at 580°C are plotted. A significant strain anisotropy of line broadening of the type $\beta_{hhh} < \beta_{h00}$ for the as-deformed state was found in both samples. This anisotropy seems to be a typical feature of these materials and was found also for milled Cu powder [13]. *Williamson-Hall* (*WH*) plots for as-prepared UFG Cu and UFG Cu + 0.5 wt.% Al_2O_3 are shown in Fig. 2. The anisotropy can be related to the dislocation-induced line broadening, and the integral breadths can be calculated using known orientation (contrast) factors for the most common slip systems in *fcc* structures (*Burgers* vector $\mathbf{b} = a/2\langle 110\rangle$). A simplified procedure for the evaluation of β is similar to that published by *Ungar et al.* [19] and it is based on Eq. (1) where D is the mean domain size in the measured direction, λ is the wavelength, Θ is the diffraction angle, k is the *Scherrer* constant, b_0 is related to stacking-fault probability, $W(g)$ is the known corresponding orientation factor, $B_0 = A_0 b\sqrt{2\ln P}$, ϱ is the dislocation density, b is the magnitude of *Burgers* vector, $A_0 \sim 1$, P is a factor related to the cut-off radius of the dislocation arrangement which must be estimated from the

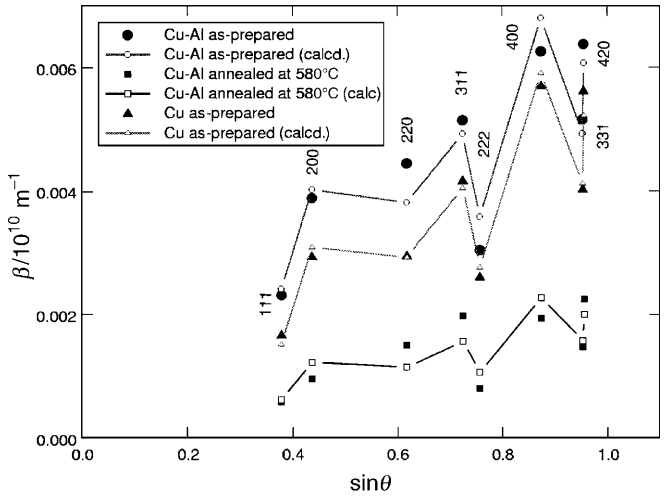

Fig. 2. *WH* plot for as-prepared pure UFG Cu (full triangles) and UFG + 0.5 wt.% Al_2O_3 in the as-prepared state (full circles) and after annealing at 580°C (full squares); calculated integral breadths are indicated by open symbols connected by solid lines

diffraction profile shape (*e.g.* from *Fourier* coefficients), and O^2 indicates non-interpreted high-order terms.

$$\beta = \frac{k}{D} + b_0 W(g) + B_0 \sqrt{\varrho} \sqrt{\langle \kappa \rangle} \frac{\sin\Theta}{\lambda} + O^2 \tag{1}$$

For a mean value of the orientation factor, the *Ungar* and *Tichy* formula (Eq. (2)) is used in such a way that the fraction of edge dislocations is weighted by w_e (Eq. (3)).

$$\langle \kappa \rangle = A + BH^2 \quad H^2 = \frac{h^2k^2 + h^2l^2 + l^2k^2}{(h^2 + k^2 + l^2)^2} \tag{2}$$

$$\langle \kappa \rangle = w_e(A_e + B_e H^2) + (1 - w_e)(A_s + B_s H^2) \tag{3}$$

The parameters A_e, B_e, A_s, and B_s for the edge and screw dislocations, respectively, can be found in Ref. [20]. A two-step procedure [13] was used to determine D, b_0, w_e, and ϱ under the assumption that the *hkl*-dependence of D and the higher-order terms O^2 can be neglected. This simplified procedure gives reasonable results, especially for the dislocation densities which are the dominant reason of line-broadening. For a more detailed analysis, a new procedure should be applied [21]. The calculated values are also shown in Fig. 2 by open symbols connected by solid lines. The agreement of experimental results and theoretical calculations is excellent. The coherent domain size a, which can be obtained from *WH* plots [22], is shown in Table 2 for both the specimens. The dislocation densities for both materials as determined by XRD are plotted in Fig. 3.

Using the diffusion model of positron behaviour in UFG materials (described in details in Ref. [5]) it is possible to calculate the linear size $2R$ of the non-distorted regions, *i.e.* the regions free of dislocations. The diffusion model can be modified

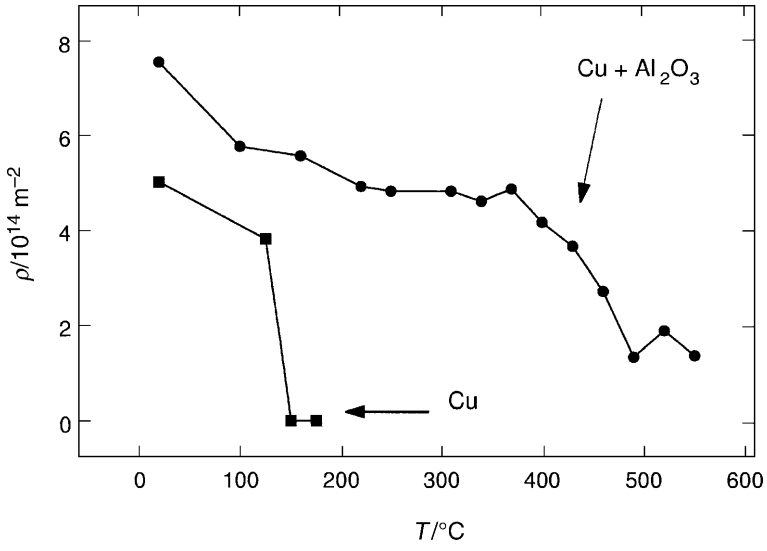

Fig. 3. Temperature dependence of the mean dislocation density determined by XRD for UFG Cu (squares) and UFG Cu + 0.5 wt.% Al_2O_3 (circles)

also to the case of saturated trapping at dislocations and microvoids which occurs in UFG Cu + 0.5 wt.% Al_2O_3. A detailed description of this modification is out of the scope of this paper and will be published separately. When applying the diffusion model to the case of saturated positron trapping in UFG Cu + 0.5 wt.% Al_2O_3, we used the additional assumption that the number of dislocations inside the distorted layers in as-prepared UFG Cu + 0.5 wt.% Al_2O_3 is the same as in pure UFG Cu. This seems to be reasonable due to the same procedure of preparation. Moreover, we can make a very simple estimation of dislocation density inside the distorted regions from the mean dislocation densities determined by XRD (Fig. 3). It is clear from Fig. 3 that the mean dislocation density in UFG Cu with Al_2O_3 exceeds that in pure UFG Cu by a factor of about 1.5. This is clearly due to the smaller domain size in the case of the UFG Cu with Al_2O_3 and, thereby, the increased volume fraction η of the distorted regions. Neglecting the dislocation density inside grain interiors, which is more than two order of magnitude smaller [5], the mean dislocation density can be expressed by Eq. (4) where η denotes the volume fraction of the distorted regions and ϱ_D is the dislocation density inside the distorted regions. If the dislocation density ϱ_D is the same in both samples, the volume fraction of the distorted regions has to be higher for UFG Cu with Al_2O_3 by the same factor as the mean dislocation density. Assuming spherical grains, the volume fraction of the distorted regions is given by Eq. (5) where a is the coherent domain size and δ denotes the thickness of the distorted regions. Using the domain sizes determined by XRD (Table 2) and $\delta = 10$ nm [3], we obtained a value of η for UFG Cu with Al_2O_3 which is higher by factor of 1.4 than η for pure UFG Cu. Thus, the XRD data also indicate that the dislocation density inside the distorted regions is virtually the same in both materials.

$$\varrho = \eta \varrho_D \tag{4}$$

$$\eta = \frac{(a+\delta)^3 - (a)^3}{(a+\delta)^3} \tag{5}$$

According to our previous results on UFG Cu [5] and TEM studies of UFG Cu [4] and UFG Cu + 0.5 wt.% Al_2O_3 [12], we further assume that the dislocation density inside the distorted regions does not change with temperature and that practically unchanged distorted regions are consumed by the recrystallizing grains during the recovery process. Using these assumptions, it is possible to obtain the volume fraction of the distorted regions (η), the size of the non-distorted regions ($2R$), and the concentration of the microvoids (c_v), also in the case of saturated positron trapping. The sizes of the non-distorted regions for both specimens calculated using the model from measured PL spectra for as-prepared UFG-Cu and UFG Cu + 0.5 wt.% Al_2O_3 are given in Table 2. They correspond well to the domain size obtained by XRD, which is confirmed also by the values in Table 2, and both quantities are very closely related to the grain sizes in the specimen. It has been found that the domain size (or size of the non-distorted regions) is slightly smaller than the mean grain size determined by TEM [4, 5]. This results from the fact that the former quantities are correlated with different dislocation densities inside the grains and inside the distorted layers along GBs, whereas the grain size is determined from different contrasts for grains and GBs in the TEM image; for more detailed discussion, see Refs. [4, 5]. The difference between these quantities obviously decreases with annealing temperature due to a change of non-equilibrium GBs to the equilibrium ones. One can see from the Table 2 that UFG Cu + 0.5 wt.% Al_2O_3 exhibits smaller grain sizes than pure UFG Cu, despite of the same preparation procedure.

Evolution of structure with temperature

It is known that the mean positron lifetime $\bar{\tau}$ is a robust parameter which does not depend on the number of components to which a PL spectrum is decomposed. Therefore, we used this parameter for the description of changes occuring during isochronal annealing of UFG Cu and UFG Cu + 0.5 wt.% Al_2O_3. The dependence of $\bar{\tau}$ on the annealing temperature for both the samples is shown in Fig. 4. One can see that $\bar{\tau}$ for UFG Cu + 0.5 wt.% Al_2O_3 is remarkably higher than for pure UFG Cu due to higher number of microvoids in UFG Cu + 0.5 wt.% Al_2O_3. Moreover, in contrast to the pure UFG Cu, it continuously increases up to 400°C. In the case of the pure UFG Cu, $\bar{\tau}$ starts to decrease at 370°C, whereas in the case of UFG Cu + 0.5 wt.% Al_2O_3 the decrease starts at 400°C, *i.e.* at a similar temperature.

The temperature dependence of the lifetimes of individual components for UFG Cu and UFG Cu + 0.5 wt.% Al_2O_3 is shown in Fig. 5; the corresponding relative intensities are plotted in Fig. 6. As one can see from Figs. 5 and 6, no free positron component was observed in UFG Cu + 0.5 wt.% Al_2O_3 up to a temperature of 430°C. On the other hand, a continuous increase of intensity I_1 takes place in pure UFG Cu from 160°C (Fig. 6), and strong increase of this intensity occurs above 370°C. This difference clearly indicates that the recovery of defects is much more pronounced in pure UFG Cu compared to UFG with Al_2O_3, *i.e.* the presence of the Al_2O_3 nanoparticles prevents the recovery of defects.

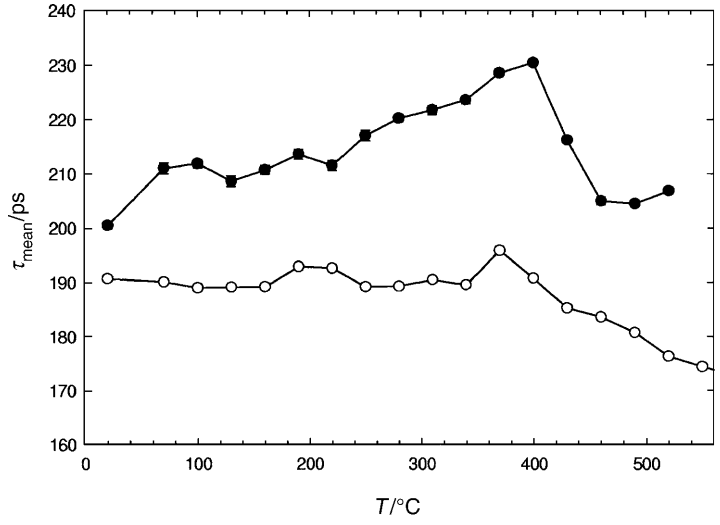

Fig. 4. Temperature dependence of the mean positron lifetime for UFG Cu (open circles) and UFG Cu + 0.5 wt.% Al_2O_3 (full circles)

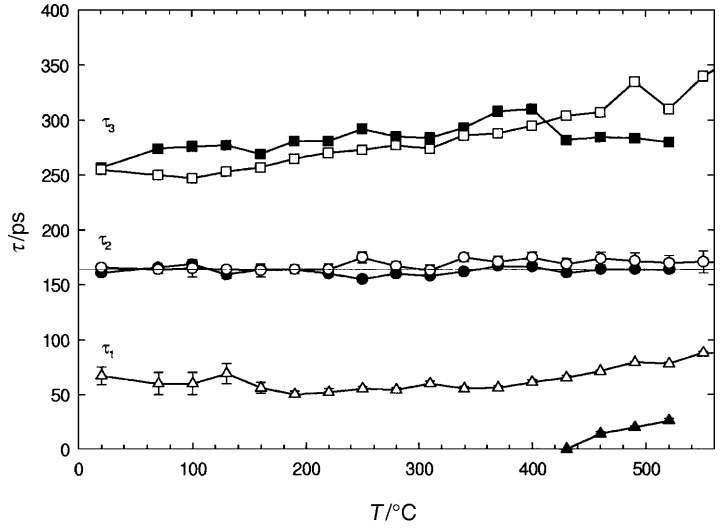

Fig. 5. Lifetimes of the components determined from PL spectra of UFG Cu (open symbols) and UFG Cu with 0.5 wt.% Al_2O_3 (full symbols) as a function of annealing temperature

The behaviour of the lifetimes τ_2 and τ_3 with temperature is practically the same for both samples (Fig. 5). Thus, the same kind of defects, *i.e.* dislocations in the distorted regions and the microvoids inside the grains, are present in both samples. The difference between the two samples consists in different concentration of these defects as well as different temperature intervals of their recovery.

The lifetime τ_2 of positrons trapped at dislocations exhibits no change with temperature. The intensity of this component starts to decrease from 160°C in pure

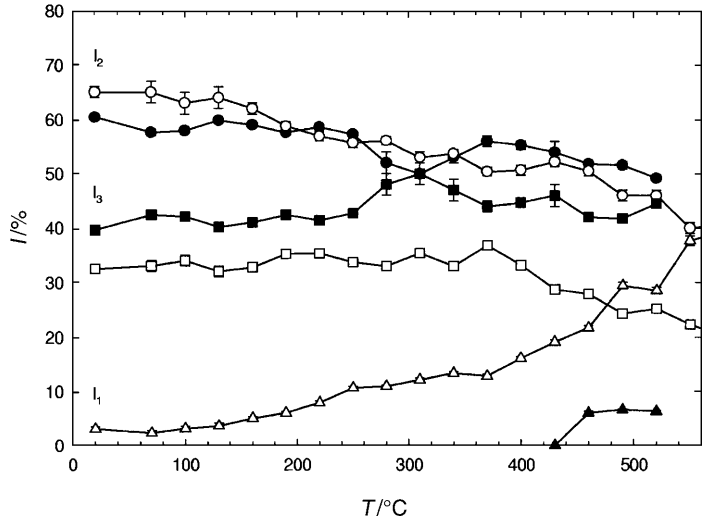

Fig. 6. Relative intensities of the components determined from PL spectra of UFG Cu (open symbols) and UFG Cu with 0.5 wt.% Al_2O_3 (full symbols) as a function of annealing temperature

UFG Cu and is correlated with an increase of the intensity I_1 of the free positron component. TEM investigations revealed an onset of the grain growth in this temperature region [4].

On the other hand, a decrease of I_2 takes place from 250°C in UFG Cu + 0.5 wt.% Al_2O_3 and, contrary to pure UFG Cu, is not accompanied by an appearance of the free positron component. This means that no recrystallized defect-free grains are formed. The decrease of I_2 in both specimens obviously reflects the recovery of the distorted regions, and one can conclude that the presence of the Al_2O_3 nanoparticles shifts the start of this recovery by about 100°C to higher temperatures.

The lifetime τ_3 of the microvoid exhibits a continuous increase with temperature for both the samples (Fig. 5), indicating that the mean size of the microvoids increases with temperature. Using theoretical calculations performed in Ref. [5], one can determine the size of the microvoids from τ_3. The temperature dependences of the size and the effective diameter of the microvoids for both specimens are plotted in Fig. 7. One can see that the initial size of the microvoids corresponds to 5 vacancies and increases to about 10 at 450°C in pure UFG Cu. The increase of size of the microvoids is less pronounced in UFG Cu + 0.5 wt.% Al_2O_3.

The relative intensity I_3 exhibits a decrease from about 370°C in pure UFG Cu. In the case of UFG Cu + 0.5 wt.% Al_2O_3 it increases from 250°C to 300°C because of the normalization of the relative intensities $I_1 + I_2 + I_3 = 100\%$ and the fact that in this temperature range $I_1 = 0\%$. The increase of I_3 is, therefore, due to the corresponding decrease of I_2 and does not indicate an increase of the number of the microvoids in this temperature interval. A determination of the concentration of the microvoids must be performed using the positron diffusion model. However, after the increase, I_3 decreases again, accompanied by the appearance of the free positron component I_1.

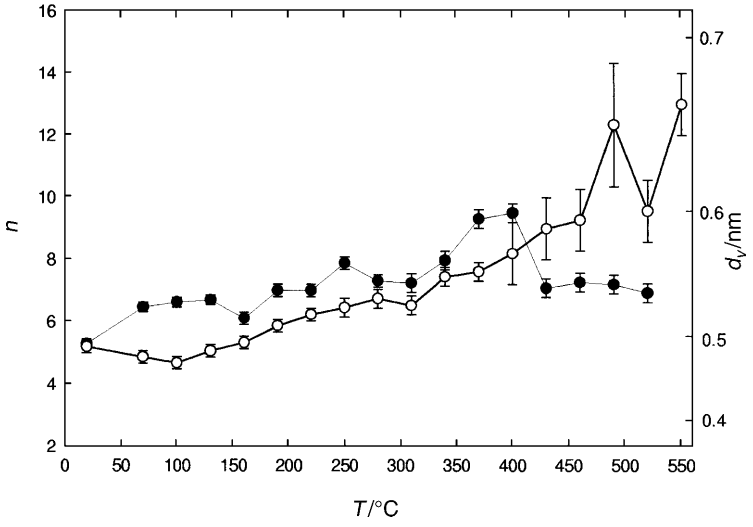

Fig. 7. Size n (in number of vacancies) of the microvoids as a function of annealing temperature for UFG Cu (open symbols) and UFG Cu + 0.5 wt.% Al_2O_3 (full symbols); the size was calculated using results from Ref. [5]; the effective diameter d_v of the microvoids is shown on the right y-axis

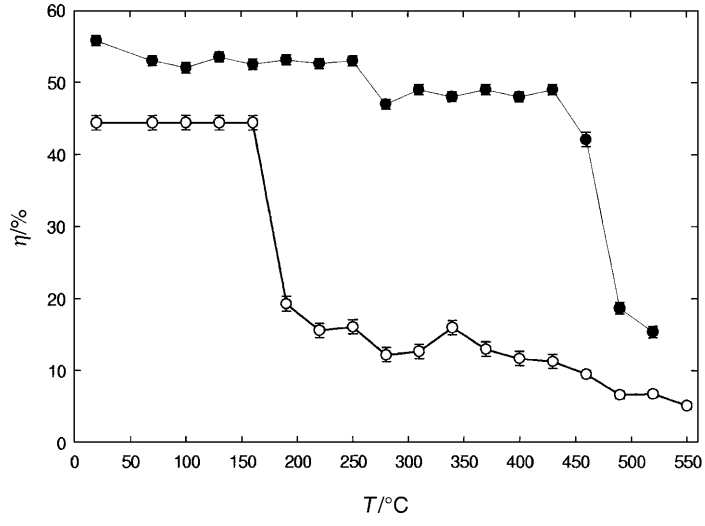

Fig. 8. Temperature dependence of the volume fraction of the distorted regions for pure UFG Cu (open circles) and UFG with 0.5 wt.% Al_2O_3 (full circles)

A further elaboration of PL spectra was performed using the diffusion model of positron behaviour in UFG materials [5, 10]. The temperature dependence of the volume fraction of the distorted regions η is plotted in Fig. 8. The higher initial volume fraction of the distorted regions in UFG Cu with Al_2O_3 is obviously due to the smaller grain size as compared to pure UFG Cu (Table 2) and the estimation performed above. In the case of pure UFG Cu, η radically decreases from 160°C to 250°C; TEM investigations have revealed that rapid grain growth takes place in

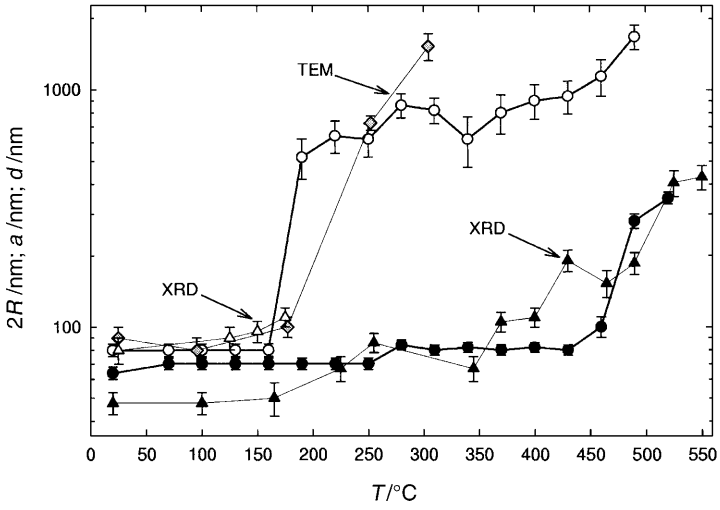

Fig. 9. Temperature dependence of the linear size of the non-distorted regions, $2R$, as determined from PL data using the diffusion model [5]; full circles: UFG Cu with Al_2O_3, open circles: pure UFG Cu; domain size a as determined by XRD for UFG Cu with Al_2O_3 (full triangles) and pure UFG Cu (open triangles); the temperature dependence of the mean grain size obtained by TEM for pure UFG Cu [4] is also included in the figure (gray diamonds)

this temperature region [4]. Thus, the recrystallization occurs in this temperature interval, as also confirmed by an analysis of the activation energy of this process [23]. Only a small decrease of η occurs in UFG Cu with Al_2O_3 in temperature region of 250–300°C, *i.e.* at about 100°C higher temperatures. The radical decrease of η taking place at 430°C reflects clearly the recrystallization in UFG Cu with Al_2O_3.

The mean sizes of the non-distorted regions (dislocation-free grain interiors), $2R$, determined using the diffusion model for both materials are shown in Fig. 9. Clearly, $2R$ exhibits good agreement with the domain size a determined by XRD (Fig. 9, full triangles). One can see from Fig. 9 that $2R$ increases rapidly from 80 nm to 500 nm during the recrystallization in the pure UFG Cu, corresponding well with TEM results [4]. On the other hand, there is only a very small increase of the mean grain size in the temperature region of 250–300°C in UFG Cu + 0.5 wt.% Al_2O_3. The most probable explanation for this fact is that only a small fraction of grains exhibits growth, *i.e.* only a few recrystallized grains appear in the deformed matrix. The recrystallization takes place from 430°C in UFG Cu with Al_2O_3 (Fig. 9) and leads to a rapid increase of grain size in the whole volume, accompanied by a decrease of the volume fraction of the distorted regions (Fig. 8). It is consistent with recent TEM results [12] which have shown that the fraction of the recrystallized grains at 400°C is not higher than 5–6%; after annealing at 600°C, it amounts to 90%. The coherent domain size lies well below 100 nm up to 400°C (Fig. 9). The mean grain size determined by TEM in Ref. [12] is still below 100 nm at 400°C in UFG Cu + 0.5 wt.% Al_2O_3, whereas it is about 1 μm, *i.e.* one order of magnitude higher, in pure UFG Cu. Thus, in agreement with Ref. [12], we can conclude

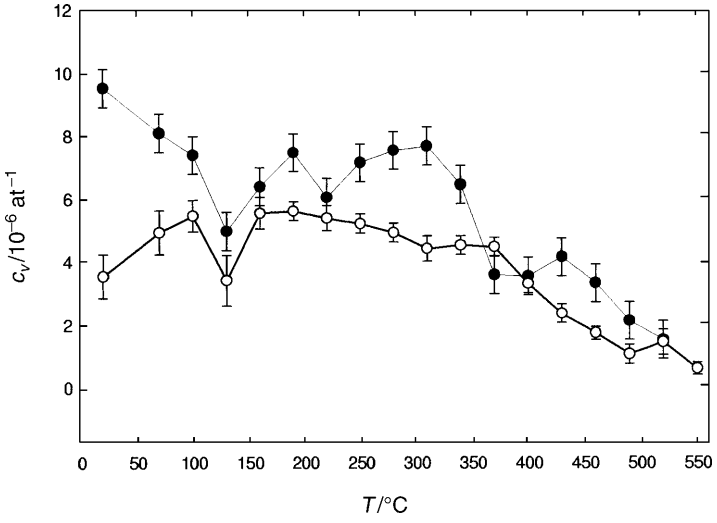

Fig. 10. Temperature dependence of concentration of the microvoids calculated from PL data using the diffusion model [5]; full symbols: UFG Cu with Al_2O_3, open symbols: pure UFG Cu

that the grain growth is substantially prevented by the presence of the Al_2O_3 nanoparticles in UFG Cu.

The concentration of the microvoids c_v can be obtained from the positron diffusion model [5, 10] and is plotted in Fig. 10. It should be noted that PL spectroscopy represents a unique tool for the investigation of the behaviour of the microvoids which are hardly detectable by other techniques. One can see from Fig. 10 that the concentration of the microvoids is higher in UFG Cu with Al_2O_3 than in pure UFG Cu. At low temperatures (below 150°C), c_v exhibits some decrease in UFG Cu + 0.5 wt.% Al_2O_3; no such behaviour occurs in pure UFG Cu. During the recrystallization in pure UFG Cu, c_v only moderately decreases. A rapid decrease starts at 370°C, *i.e.* in already recrystallized UFG Cu. In the case of UFG Cu + 0.5 wt.% Al_2O_3, c_v exhibits a decrease from 300°C, *i.e.* prior to recrystallization, and a further decrease takes place above 400°C during recrystallization. In general, the behaviour of the microvoids with annealing temperature is relatively similar in both specimens, despite of completely different temperature regions of the recrystallization.

Conclusions

The results obtained in the present work can be summarized into the following items:

(*i*) The decrease of the mean dislocation density, which is caused by the decrease of the volume fraction of the distorted regions along GBs, is shifted to significantly higher temperatures in UFG Cu with 0.5 wt.% Al_2O_3. The recrystallization occurs in the temperature region of 160–250°C in pure UFG Cu, whereas in UFG Cu with 0.5 wt.% Al_2O_3 it starts above 400°C. The mean grain size in UFG Cu with 0.5 wt.% Al_2O_3 remains below 100 nm up to 400°C.

(*ii*) UFG Cu with 0.5 wt.% Al_2O_3 contains a higher number of microvoids than pure UFG Cu. The behaviour of the microvoids with annealing temperature is similar in both materials.

Experimental

Specimens

Pure copper of purity 99.99% and a mixture of copper (99.9%) with 0.5 wt.% Al_2O_3 nanoparticles (GlidCop Al-15) were studied. In order to fabricate the UFG structure, the specimens were subjected to HPT at 6 GPa and room temperature. The true logarithmic strain can be expressed as $e = \ln(\theta r/l)$, where θ is the rotation angle in radians, and r and l are the radius and thickness of the disk, respectively [3]. In our case, $e = 7$, which corresponds to 7 rotations. The HPT technique has been described in detail in Refs. [1–3]. The microstructure of the as-prepared state of the specimens was investigated by PL and XRD spectroscopy. Subsequently, the specimens were subjected to isochronal annealing. The temperature step was choosen as 30°C, and specimens were annealed for 30 min at each temperature, *i.e.* the corresponding effective heating rate was 1°C/min. The annealing was carried in an oil base thermostat up to 250°C and in a vertical furnace with a protective argon atmosphere above this temperature. Each annealing step was finished by quenching with water of room temperature. Both PL and XRD measurements were performed at room temperature.

Positron lifetime spectroscopy

A PL spectrometer as described in Refs. [24, 25] was employed in the present work. A ^{22}Na positron source (activity: ~1.3 MBq) sealed between two mylar foils (thickness: 2 μm) was used. The timing resolution of the spectrometer was 160 ps (FWHM) for ^{22}Na at a typical coincidence counting rate of ~80 s^{-1}. At least 10^7 counts were collected in each PL spectrum. The measured spectra were decomposed by employing the maximum-likelihood procedure [26].

X-Ray diffraction

X-Ray studies were carried out using XRD7 and HZG4 (Seifert-FPM) powder diffractometers (CuK_α radiation filtered with a nickel foil, *Soller* slits placed in the diffracted beam). XRD profiles were fitted with the *Pearson* VII function by the program DIFPATAN [27]. XRD line broadening was evaluated by integral breadths (β) and FWHMs in terms of the WH plots (β *vs.* sinθ). The correction for instrumental broadening was performed with the aid of a NIST LaB_6 standard and the *Voigt* function method. Then, the modified *WH* method was used for the determination of coherent domain size and dislocation density (lattice microstrains).

Acknowledgements

This work was supported by the Czech Ministry of Education, Youth and Sport (project COST OC 523.50). The residency of *Jakub Čížek* at the University of Göttingen is supported by the *Alexander von Humboldt* Foundation.

References

[1] Valiev RZ (1997) Mat Sci Eng A **234–236**: 59
[2] Valiev RZ (1995) Nanostructured Mater **6**: 73
[3] Valiev RZ, Islamgaliev RK, Alexandrov IV (2000) Progress in Materials Science **45**: 103

[4] Islamgaliev RK, Chmelík F, Kužel R (1997) Mat Sci Eng A **237**: 43
[5] Čížek J, Procházka I, Cieslar M, Kužel R, Kuriplach J, Chmelík F, Stulíková I, Bečvář F, Melikhova O, Islamgaliev RK (2002) Phys Rev B (in press)
[6] Alexandrov IV, Zhang K, Kilmametov AR, Lu K, Lu BZ, Valiev RZ (1997) Mat Sci Eng A **234**–**236**: 331
[7] Valiev RZ, Musalimov RS, Tsenev NK (1989) Phys Stat Sol (A) **115**: 451
[8] Valiev RZ, Alexandrov IV, Islamgaliev RK (1998) In: Chow GM, Noskova NI (eds) Nanocrystalline Materials: Science and Technology, NATO ASI. Kluwer, p 121
[9] Valiev RZ, Islamgaliev RK (1998) In: Ghosh AK, Bieler TR (eds) Superplasticity and Superplastic Forming 1998. The Minerals, Metals and Material Society, p 117
[10] Čížek J, Procházka I, Vostrý P, Chmelík F, Islamgaliev RK (1999) Acta Phys Pol A **95**: 487
[11] Islamgaliev RK, Amirkhanov NM, Bucki JJ, Kurzydlowski KJ (2000) In: Lowe TC, Valiev RZ (eds) Investigations and Applications of Severe Plastic Deformation, NATO Science Series 3: High Technology 80. Kluwer, p 297
[12] Buchgraber W, Islamgaliev RK, Kolobov YUR, Amirkhanov NM (1999) In: NATO ARW. Moscow August 2–9, 1999
[13] Kužel R, Čížek J, Procházka I, Chmelík F, Islamgaliev RK, Amirkhanov NM (2001) In: METAL 2001. Ostrava, Tanger Ltd (CD ROM)
[14] Hautojärvi P, Corbel C (1995) In: Dupasquier A, Mills AP (eds) Proceedings of the International School of Physics ''Enrico Fermi'', Course CXXV. IOS Press, Varenna, p 491
[15] McKee BTA, Saimoto S, Stewart AT, Scott MJ (1974) Can J Phys **52**: 759
[16] de Lima AP, Lopes Gil C, Martins DR, Ayres de Campos N, Menezes LF, Fernandes JV (1987) In: Dlubek G, Brümmer O, Brauer G, Hennig K (eds) Proceedings od European Meeting on Positron Studies of Defects, vol. 2, part 1. Martin-Luther-Universität Halle-Wittenberg, Wernigerode, p C1
[17] Dupasquier A, Romero R, Somoza A (1993) Phys Rev B **48**: 9235
[18] PDF-2, Powder Diffraction Pattern Database, ICDD (International Centre for Diffraction Data), record number 04-0836
[19] Ungár T, Dragomir I, Revesz I, Borbely A (1999) J Appl Cryst **32**: 992
[20] Ungár T, Tichy G (1999) Phys Stat Sol (B) **171**: 425
[21] Ungár T, Gubiza J, Ribárik G, Borbély A (2001) J Appl Cryst **34**: 298
[22] Kužel R, Čížek J, Procházka I, Chmelík F, Islamgaliev RK, Amirkhanov NM (2001) Mat Sci Forum **378**–**381**: 463
[23] Čížek J (2001) PhD Thesis, Charles University, Prague, Czech Republic
[24] Bečvář F, Čížek J, Lešták L, Novotný I, Procházka I, Šebesta F (2000) Nucl Instr Meth A **443**: 557
[25] Bečvář F, Čížek J, Procházka I (1999) Acta Physica Polonica A **95**: 448
[26] Procházka I, Novotný I, Bečvář F (1997) Mat Sci Forum **255**–**257**: 772
[27] Kužel R (1995) DIFPATAN – Program for Powder Pattern Analysis, http://www.xray.cz/priv/kuzel/difpatan

Received October 5, 2001. Accepted (revised) December 20, 2001